

Observation of magnetic fluctuations and rapid density decay of magnetospheric plasma in Ring Trap 1

H. Saitoh, Z. Yoshida, J. Morikawa, Y. Yano, H. Mikami, N. Kasaoka, and W. Sakamoto
 Graduate School of Frontier Sciences, University of Tokyo, 5-1-5 Kashiwanoha, Kashiwa,
 Chiba 277-8561, Japan

(Received 13 February 2012; accepted 2 May 2012; published online 12 June 2012)

The Ring Trap 1 device, a magnetospheric configuration generated by a levitated dipole field magnet, has created high- β (local $\beta \sim 70\%$) plasma by using electron cyclotron resonance heating (ECH). When a large population of energetic electrons is generated at low neutral gas pressure operation, high frequency magnetic fluctuations are observed. When the fluctuations are strongly excited, rapid loss of plasma was simultaneously observed especially in a quiet decay phase after the ECH microwave power is turned off. Although the plasma is confined in a strongly inhomogeneous dipole field configuration, the frequency spectra of the fluctuations have sharp frequency peaks, implying spatially localized sources of the fluctuations. The fluctuations are stabilized by decreasing the hot electron component below approximately 40%, realizing stable high- β confinement. © 2012 American Institute of Physics. [<http://dx.doi.org/10.1063/1.4728089>]

The Ring Trap 1 (RT-1) device^{1,2} is a magnetospheric dipole field configuration constructed for the studies of high- β plasma suitable for burning advanced fuels.¹⁻⁴ The dipole fusion concept³ was motivated by a natural example of high- β plasma observed in the Jovian magnetosphere.⁵ Although plasma is trapped in bad curvature regions, it was pointed out that the dipole plasmas can be stable against MHD interchange and ballooning instabilities due to the effects of plasma compressibility³ and magnetic separatrix.⁶ Intensive studies on high- β plasmas in the magnetospheric configurations have been conducted on RT-1,¹ Mini-RT,⁷ and levitated dipole experiment (LDX)⁸ by using levitated superconducting magnets. In the first series of experiments in RT-1, plasma is generated and maintained by using electron cyclotron resonance heating (ECH). High- β hot-electron plasma has been successfully realized in RT-1 (Ref. 9) through the optimization of formation conditions including the feedback-controlled levitation of the dipole field magnet.¹⁰

In the presence of intense energetic charged particles in plasmas, emergence of several kinds of fluctuations and instabilities are widely observed.¹¹⁻¹⁷ Existence of multiple temperature components and velocity space anisotropy in the plasma can be energy sources for the onset of instabilities.¹⁸ Understanding of the stability limit and fluctuation properties is very important for the realization of stable confinement of high- β plasma in the magnetospheric configuration. In this brief communication, we report the observation of MHz-range magnetic fluctuations in RT-1, which emerge when the population of energetic electrons is very large. Experimental investigations on the spatial structures and conditions for the excitation of the fluctuations are reported.

Figure 1 schematically shows the vacuum chamber, magnetic surfaces, and diagnostics of RT-1. A superconducting (Bi-2223) dipole field magnet is located inside the chamber and can be magnetically levitated by using a lifting magnet positioned at the top of the chamber.² In the present experiment, however, the dipole field magnet was mechani-

cally supported, and plasma was confined in a pure dipole field configuration. Hydrogen plasma was generated and heated by ECH using 2.45 GHz microwave with 1 s duration. Diamagnetic signals and plasma pressure were measured by magnetic loops wound outside of the chamber and Hall sensors located inside the chamber. A 75 GHz (4 mm) interferometer was installed at tangential ports (Fig. 1(a)) and used for the measurements of electron line density. The tangency radius of the interferometer chord was $r_{\text{int}} = 45$ cm, which was close to the radial position $r_{\text{ECR}} = 44$ cm of 2.45 GHz electron cyclotron resonance layer on the midplane. Si(Li) detectors and edge Langmuir probes were used for the measurements of electron temperature. More detailed descriptions on RT-1 and the diagnostic system are presented in Refs. 7 and 9 and references therein.

For the measurements of magnetic fluctuations, pickup coils (B dot probes) were installed at north ports (1 and 2), at a northwest (NW) port (3), and at a southwest (SW) port (4) of RT-1 as shown in Fig. 1. The pickup coils 1, 3, and 4 were located at the equator of the chamber ($z = 0$ cm) at $r = 97$ cm. The pickup coil 2 was located at $r = 95$ cm and $z = 12$ cm, so that coils 1 and 2 were approximately located on a same field line. Typical field strength at the coil positions was 5×10^{-3} T. In order to subtract the electrostatic component of fluctuations caused by a stray capacitance between the pickup coil and plasma, the probe tip consisted of differential pair of three-turn loops wound around a 10×10 mm polytetrafluoroethylene (PTFE) rod. This creates equal but opposite polarity of magnetic signals, and same polarity signals of electrostatic components. We found that the capacitive coupling between the pickup coil and plasma was relatively small, and typical strength ratio of the electric and magnetic field fluctuations detected by the magnetic coil, \tilde{E}/\tilde{B} , was less than 5%. Each of the pickup coils was positioned to measure the z component of magnetic fluctuations. The fluctuation signals were recorded by a 500 MHz broadband oscilloscope and were converted into frequency spectra

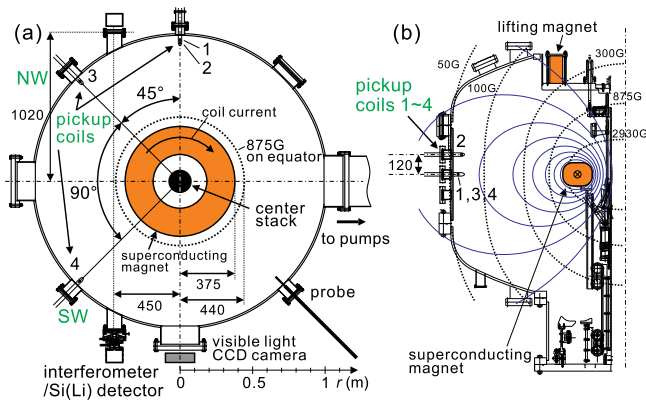


FIG. 1. (a) Top view and (b) projection on the poloidal cross section of the RT-1 experiment including the locations of magnetic pickup coils. Thin lines show magnetic surfaces and field strength contours generated by a dipole field magnet.

with a conventional short-time fast Fourier transform (FFT) method.

In the plasma of RT-1 generated by ECH, measurements with x-ray detectors and edge Langmuir probes showed that electrons have multiple temperature components. The typical temperatures of the hot electron component are 30 keV when the dipole field magnet was levitated and 10 keV when the magnet was not levitated. Plasma pressure in the present experiments is mainly attributed to the hot electrons. Due to their small cross sections of collisions with other particles, the hot electrons have long confinement time. As a result, electron densities observed by the interferometer decrease with different time constants after the stop of microwave injection. The initial rapid decrease is due to the loss of cold electrons of ~ 10 eV, and the second slow decay is due to the effects of long-lived hot electrons.⁹ By decreasing neutral gas pressure, very intense hot electrons are generated. In such cases, the plasma becomes unstable and the excitation of MHz range magnetic fluctuations was observed.

Figure 2 shows the typical temporal evolution of plasma and the burst of magnetic fluctuation emerged in a slow decay phase after the microwave was turned off. Similar onset of magnetic fluctuations and rapid density decay were also observed in the heating phase when the neutral gas pressure was below ~ 0.5 mPa. After the stop of microwave power at $t = 0$ s (Fig. 2(a)), the plasma started to decay. Significant magnetic fluctuations were not observed at this period, and the plasma was in a quiet state. The onset of small fluctuation was observed at $t = 2.35$ ms (Fig. 2(d)), but there was no major change in the decay rate of line averaged electron density n_{ave} (Fig. 2(b)). Following the rapid growth of fluctuation amplitude at $t = 2.58$ ms, a temporary increase in n_{ave} and disruptive density loss was observed at $t = 2.59$ ms and $t = 2.6$ ms, respectively. Here, ionizing effects due to escaping hot electrons are possible reasons for the observed increase in n_{ave} . Typical strength of the fluctuating magnetic field at this point was $\tilde{B} \sim 10^{-4}$ T. In Fig. 2(c), the diamagnetic signal shows that plasma pressure decayed slowly after the decay of n_{ave} , suggesting that a part of the hot electrons was still trapped in this period outside the chord of the interferometer.

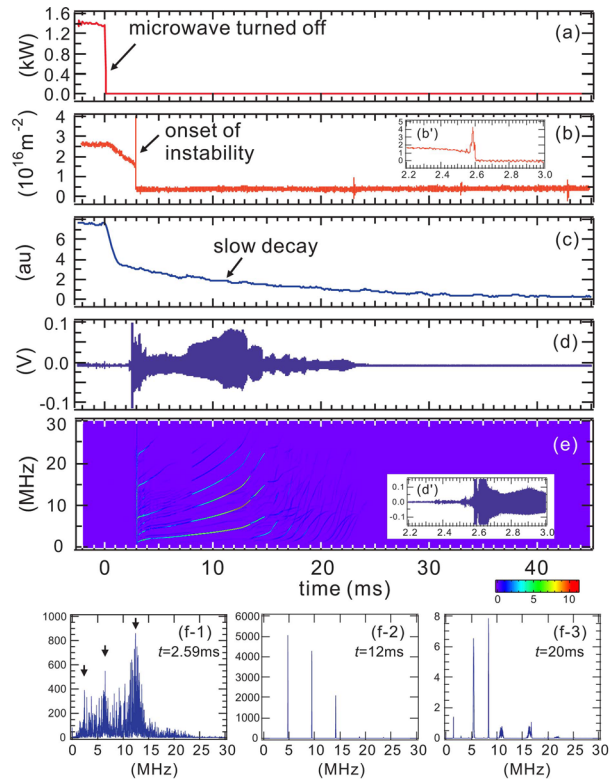


FIG. 2. Onset of fluctuation and plasma decay. (a) Input microwave power, (b) line density, (c) diamagnetic signal, (d) magnetic fluctuation measured by the pickup coil, and (e) its power spectrum. Frequency power spectra (f-1) before the decay of density, (f-2) in slow chirping phase, and (f-3) fast chirping phase.

The fluctuations had complicated frequency sweep behaviors and their frequency power spectra had several peaks as shown in Figs. 2(e) and 2(f). At $t = 2.59$ ms, just before the disruptive density loss, the power spectrum had rather broad peaks approximately centered at $f = 2.4$, 6.3, and 12.3 MHz, as shown in Fig. 2(f-1). Temporal variations of the fluctuation frequency, or chirping, with $df/dt \sim 10$ MHz/ms were repeatedly observed in the following phase. In this period, there were sharp discrete peaks in the frequency power spectrum as shown in Figs. 2(f-2) and (f-3). Although the plasma is confined in a strongly inhomogeneous dipole field configuration, the frequency spectra of the fluctuations have sharp frequency peaks. Electrostatic fluctuations in similar frequency ranges were reported in Collisionless Terrella Experiment (CTX) (Ref. 16) and LDX^{8,17} and identified as interchange instabilities excited by the effects of hot electrons.

The emergence of magnetic fluctuations that lead to disruptive plasma loss was observed only when the neutral gas pressure P_n was low and plasma pressure was sufficiently high. Figure 3 plots the line averaged electron density n_{ave} and the diamagnetic signal $\Delta\Psi$ of plasma when the large magnetic fluctuation was observed (closed triangles) and when not observed (open circles). In the present experiment, the plasma pressure was relatively low due to the mechanically supported superconducting magnet. After the stop of microwave injection, plasma decayed quietly or instability emerged during the decay phase depending on n_{ave} and $\Delta\Psi$. The fluctuation burst was not excited when the ratio of hot electron component was moderate and $\Delta\Psi$ was small,

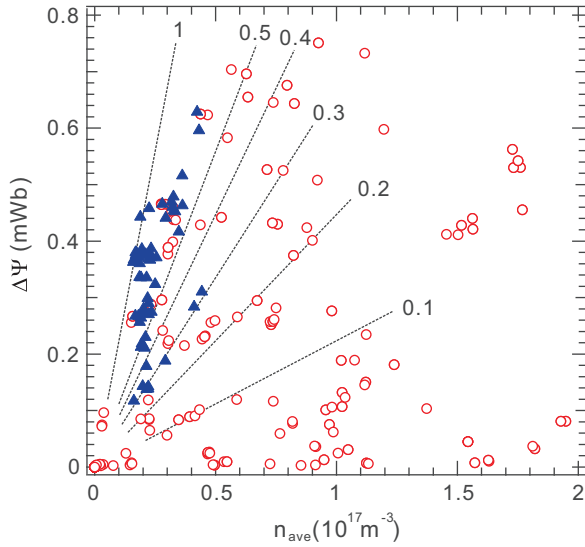


FIG. 3. Line averaged electron density n_{ave} and diamagnetic signal $\Delta\Psi$ of plasma when strong magnetic fluctuation and rapid plasma loss were observed (closed triangles) and when not observed (open circles). Dotted lines show the estimated ratio of hot electron component in the plasma.

suggesting the stabilizing effects of cold component electrons.^{18,19} By increasing input microwave power while keeping P_n lower than approximately 2 mPa, drastic increase in the hot electron component was realized, resulting the formation of plasma with low n_{ave} and large $\Delta\Psi$. In these cases, the onset of magnetic fluctuation and sudden density loss were observed in the plasma decay phase. Even when the plasma pressure was relatively high with large $\Delta\Psi$, the fluctuations were stabilized by increasing P_n , as a result of the reduced ratio of the hot electron component.

Typical bremsstrahlung x-ray energy spectrum of the plasma measured with a Si(Li) detector is shown in Fig. 4. The detector viewed the plasma through a tangential port (Fig. 1(a)). An electron temperature of $T_e = 9.2$ keV was deduced from the spectrum for the hot electron component of the plasma. Under the present experimental condition with a mechanically supported superconducting magnet and application of microwave power P_{rf} from 2 to 5 kW at $P_n \sim 2$ mPa, T_e was relatively low and did not strongly depend on P_{rf} . By a numerical analysis of plasma equilibrium using a Grad-Shafranov calculation code,⁶ we have an empirical relationship between the averaged diamagnetic signal $\Delta\Psi$ and maximum local β for

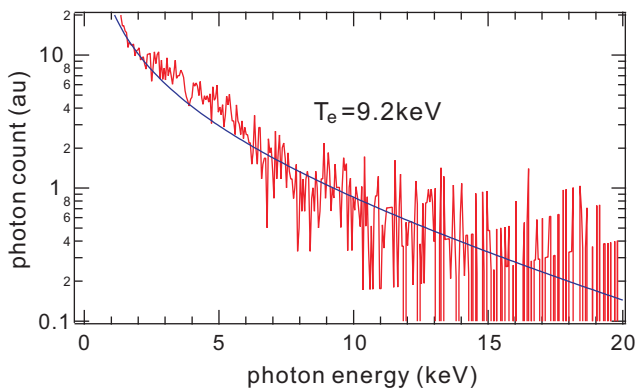


FIG. 4. Typical x-ray spectrum of plasma obtained with a Si(Li) detector.

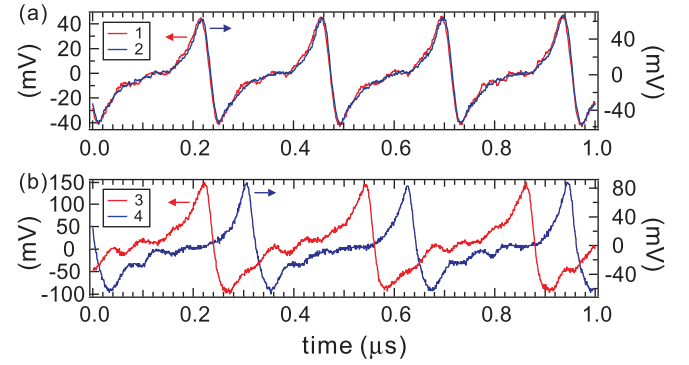


FIG. 5. Fluctuation signals observed (a) by pickup coils 1 and 2 located along same field line, and (b) by pickup coils 3 and 4 located at different toroidal positions at $z = 0$ cm. Toroidal angle difference between coils 3 and 4 was 90° (see Fig. 1(a)).

the present plasma pressure range: $\beta = 1.8 \times 10^2 \times \Delta\Psi$. By using $T_e = 9$ keV as a typical hot electron temperature and typical magnetic field strength $B = 0.03$ T in the confinement region, hot electron density n_h and $\Delta\Psi$ are related as $n_h = 4.5 \times 10^{19} \times \Delta\Psi$. Dotted lines in Fig. 3 show the ratio of the hot electron component, α , estimated by using this relationship. Here, we approximated that $\alpha \sim n_h/n_{\text{ave}}$, because the electron density has rather flat radial profiles when the dipole field magnet was not levitated.⁹ There is a strong correlation between α and the onset of instability. The strong magnetic fluctuation and rapid loss of plasma were not observed when α was below approximately 30% ~ 50%, indicating that the effects of hot electron component restrict the low neutral gas operation of the magnetospheric plasma.

Spatial mode structures of the fluctuation were measured by using two magnetic probes located at different positions. Figure 5 shows the typical waveforms of the fluctuation signals measured by poloidally (pickup coils 1 and 2 in Fig. 1) and toroidally (3 and 4) separated probes. The pickup coils 1 and 2 were located in the same poloidal cross section at $z = 0$ cm and $+12$ cm, respectively. Toroidal separation angle between the pickup coils 3 and 4 was $\theta_{34} = 90^\circ$. The

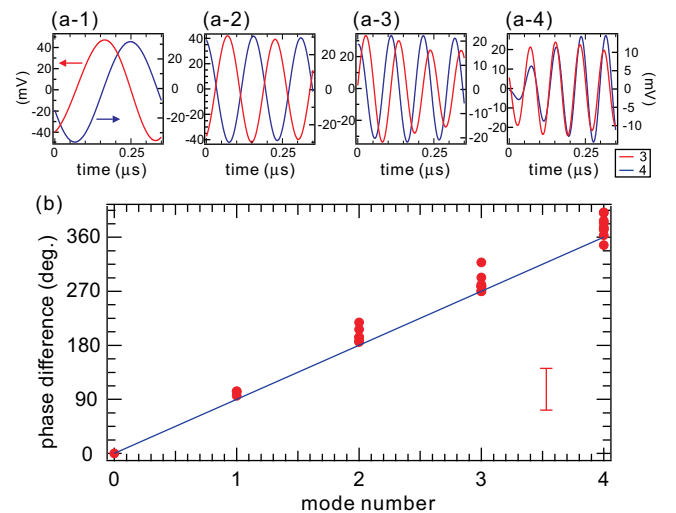


FIG. 6. (a-1) $m = 1$, (a-2) $m = 2$, (a-3) $m = 3$, and (a-4) $m = 4$ components of pickup signals 3 and 4 shown in Fig. 5(b). (b) Phase difference of each of the modes.

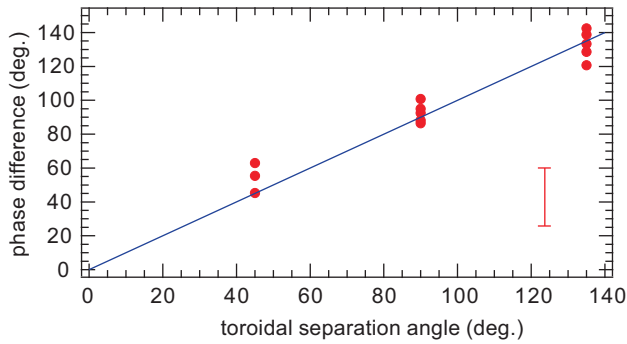


FIG. 7. Phase differences between the fluctuation signals of the lowest frequency ($k=1$) component, measured with pickup coils located with different toroidal separation angles.

fluctuation phase had very weak dependences along field lines, while clear phase differences were observed in the cross field toroidal direction. By comparing the waveforms of the pickup coils 3 and 4, we found that the propagation direction of the fluctuation agrees with the electron diamagnetic motion, also suggesting that the hot electrons are the energy source for the onset of fluctuation.

As shown in Fig. 2(f), the fluctuation frequency spectra have several peaks centered at $f=f_k$ ($k=1, 2, \dots$), and the fluctuation signals can be described by a sum of each of the frequency components as $\sum_{k=1}^n A_k \cos(2\pi f_k t - \phi_k)$, where A_k is the amplitude and ϕ_k is the phase of the components. When the fluctuations were rather stable as shown in Figs. 2(f-2) and (f-2), the peak frequencies are approximately equal to the integral multiple of the lowest peak frequency, $f_k = k f_1$. Figure 6(a) plots each of the frequency components $A_k \cos(2\pi k f_1 t - \phi_k)$ ($k=1-4$) of the fluctuation signals measured by the pickup coils 3 and 4. Phase differences between the signals of the two coils are shown in Fig. 6(b) for the frequency components of $k=1-4$. The error bars in Figs. 6 and 7 are twice the standard deviations of the measured phase values. The observed phase difference was equal to $k \times \theta_{34}$, indicating that k corresponds to the toroidal mode number m of the fluctuations. Figure 7 shows phase differences of the lowest frequency component ($k=1$) measured with the pickup coils 1, 3, and 4, located at three different toroidal positions. Possible azimuthal mode numbers are $m = 1 \pm 8n$, where n is an integer. If $n \neq 0$, the observations in Fig. 6 indicate that discrete modes ($m=9, 18, 27, 36$ if $n=1$, for example) are selectively excited in the plasma, which is physically quite improbable. In the case of $n=0$, the phase velocity of the fluctuation is in the electron diamagnetic direction. For $T_e = 10$ keV, curvature ~ 0.5 m and typical field strength ~ 0.01 T at edge confinement region, toroidal drift velocity of hot electrons is in the order of 10^6 m/s, which is comparable to the fluctuation phase velocity.

To summarize, we reported the observation of magnetic fluctuations and rapid loss of electron density in magnetospheric ECH plasma in RT-1 when the population of the hot electron component is very large. The fluctuations propagate in the toroidal direction that agrees with the electron diamagnetic drift direction. The fluctuation frequency is comparable to the toroidal drift frequency of the hot electrons, and the effects of hot electrons are possible reasons for the onset of fluctuations. Although the plasma is confined in a strongly inhomogeneous dipole field configuration, the frequency spectra of the fluctuations have sharp frequency peaks. It is possible that the sharp peaks are generated, because the sources of the fluctuations are spatially localized in the confinement region. The observed high-frequency fluctuations clearly restrict the low neutral gas pressure operation in the magnetospheric configuration. The fluctuations are suppressed by sufficient neutral gas fueling and the resultant increase in the cold electron component, realizing stable high β state.

The authors are grateful to Assoc. Prof. Masaru Furukawa for valuable comments and discussions. This work was supported by Grants-in-Aid for Scientific Research (23224014) from MEXT of Japan.

- ¹Z. Yoshida, Y. Ogawa, J. Morikawa, S. Watanabe, Y. Yano *et al.*, *Plasma Fusion Res.* **1**, 008 (2006).
- ²Y. Ogawa, Z. Yoshida, J. Morikawa, H. Saitoh, S. Watanabe *et al.*, *Plasma Fusion Res.* **4**, 020 (2009).
- ³A. Hasegawa, *Comments Plasma Phys. Controlled Fusion* **11**, 147 (1987).
- ⁴A. C. Boxer, R. Bergmann, J. L. Ellsworth, D. T. Garnier, J. Kesner, M. E. Mauel, and P. Woskov, *Nat. Phys.* **6**, 207 (2010).
- ⁵S. M. Krimigis, T. P. Armstrong, W. I. Axford, C. O. Bostrom, C. Y. Fan *et al.*, *Science* **206**, 977 (1979).
- ⁶M. Furukawa, H. Hayashi, and Z. Yoshida, *Phys. Plasmas* **17**, 022503 (2010).
- ⁷Y. Ogawa, J. Morikawa, T. Mito, N. Yanagi, M. Iwakuma *et al.*, *J. Plasma Fusion Res.* **79**, 643 (2003).
- ⁸D. T. Garnier, A. Hansen, M. E. Mauel, E. Ortiz, A. C. Boxer *et al.*, *Phys. Plasmas* **13**, 056111 (2006).
- ⁹H. Saitoh, Z. Yoshida, J. Morikawa, Y. Yano, T. Mizushima *et al.*, *Nucl. Fusion* **51**, 063034 (2011).
- ¹⁰Y. Yano, Z. Yoshida, Y. Ogawa, J. Morikawa, and H. Saitoh, *Fusion Eng. Des.* **85**, 641 (2010).
- ¹¹A. F. Kuckes, *Phys. Fluids* **9**, 2239 (1966).
- ¹²H. Ikegami, H. Ikezi, M. Hosokawa, K. Takayama, and S. Tanaka, *Phys. Fluids* **11**, 1061 (1968).
- ¹³S. Hiroe, J. B. Wilgen, F. W. Baity, L. A. Berry, R. J. Colchin *et al.*, *Phys. Fluids* **27**, 1019 (1984).
- ¹⁴R. C. Garner, M. E. Mauel, S. A. Hokin, R. S. Post, and D. L. Smatlak, *Phys. Fluids B* **2**, 242 (1990).
- ¹⁵H. P. Warren, M. E. Mauel, D. Brennan, and S. Taromina, *Phys. Plasmas* **3**, 2143 (1996).
- ¹⁶B. Levit, D. Maslovsky, and M. E. Mauel, *Phys. Plasmas* **9**, 2507 (2002).
- ¹⁷E. E. Ortiz, A. C. Boxer, J. L. Ellsworth, D. T. Garnier, A. K. Hansen *et al.*, *J. Fusion Energy* **26**, 139 (2007).
- ¹⁸A. Hasegawa, *Plasma Instabilities and Nonlinear Effects* (Springer-Verlag, 1975).
- ¹⁹N. A. Krall, *Phys. Fluids* **9**, 820 (1966).